

Conduction Modes of a Peak Limiting Current Mode Controlled Buck Converter

Predrag Pejović and Marija Glišić

Abstract—In this paper, analysis of a buck converter operated applying a peak limiting current mode control is performed, focusing regions where the limit cycle is unstable. Normalized discrete time converter model is derived. Chart of operating modes is presented, and it is shown that the converter exhibits an infinite number of discontinuous conduction modes in an area where the continuous conduction mode would be expected assuming stable limit cycle. The converter is analyzed applying numerical techniques to determine period number of different discontinuous conduction modes and dependence of the output current on the output voltage and the limiting current. The numerical results agree with the analytical results in areas where the limit cycle is stable, and differ in regions where the limit cycle is unstable. Two different notions of stability, the limit cycle stability and the converter open loop stability, are clarified.

Index Terms—Buck Converter, Current Mode Control, Discontinuous Conduction Mode.

I. INTRODUCTION

Buck converter, shown in Fig. 1, operated applying the peak limiting current mode control is analyzed in this paper, aiming proper understanding and modeling of regions characterized by unstable limit cycle. Analytical models of buck converters are presented in [1], where both the continuous and the discontinuous conduction mode are analyzed, as well as instability of the limit cycle in the continuous conduction mode for the output voltage greater than one half of the input voltage. The results presented there indicate open loop instability of the converter in the discontinuous conduction mode for the output voltage greater than one half of the input voltage, although the limit cycle should be stable in this case. Comprehensive presentation of [1] aggregates results of many previous publications. Although the topic is more than 30 years old [2], it occasionally attracted attention over decades [3-7]. Detailed analysis is presented in [6], where fairly general case is analyzed, resulting in equations that are sometimes hard to follow. Discrete time model of the converter and bifurcations are analyzed in [7]. In [8], open loop instability of the converter operated in the discontinuous conduction mode for the output voltage greater than one half of the input voltage is analyzed, and as an auxiliary result multiple period discontinuous conduction modes are noticed. Besides, such waveforms have been occasionally observed in practice, but remained without a deeper analysis. This paper is a continuation of [8], focusing regions of unstable limit cycle operation.

Purpose of this paper is to clarify operation of the peak limiting current mode controlled buck converter in regions where the limit cycle is unstable in an easy-to-follow manner. To

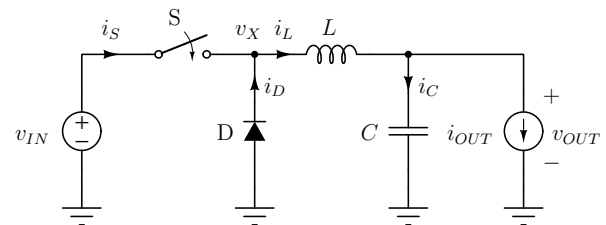


Fig. 1. Buck converter.

achieve this goal, both analytical and numerical techniques are applied. Analysis of the buck converter is reduced to analysis of a switching cell. The circuit voltages, currents, and time are normalized to generalize the results. A program to analyze the switching cell operation is given, and the results obtained using the program are presented, analyzed and discussed. It is shown that the converter exhibits an infinite number of period- n discontinuous conduction modes, and boundaries of the region where such modes exist are analytically derived. Regions where period- n discontinuous conduction modes occur are determined numerically and presented for $n \leq 10$. Dependence of the converter output current on the output voltage and the limiting current is computed numerically, and the results are equal to theoretical predictions in the regions where period-1 operation occurs, while different elsewhere. Open loop stability of the converter, being a concept different than the limit cycle stability, is analyzed numerically, and unstable regions are identified.

II. REDUCTION TO A SWITCHING CELL MODEL

A. Approximation

To simplify the analysis and to focus attention to the part of the circuit that causes the complex behavior, let us assume that the converter output voltage is constant. This assumption at least has to hold over one switching period, to justify linear ripple approximation. The assumption results in a simplified equivalent circuit of the buck converter, as shown in Fig. 2, frequently named as a “switching cell”.

B. Circuit Equations

After the converter is reduced to the switching cell introducing the approximation that the output voltage is constant, solving the circuit essentially reduces to determination of the inductor current waveform. Governing equation to determine the inductor current waveform is

$$L \frac{di_L}{dt} = v_L \quad (1)$$

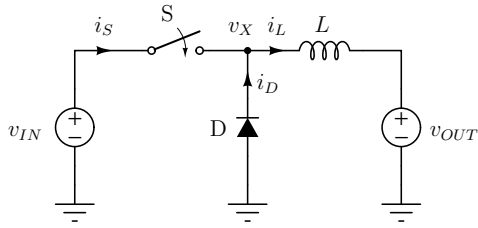


Fig. 2. Switching cell.

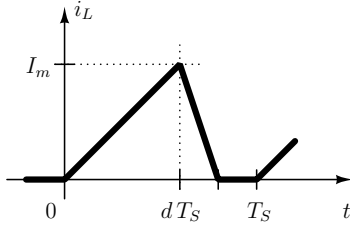


Fig. 3. Aimed waveform of i_L in the DCM.

which is a differential equation that requires an initial condition to provide a unique solution.

Voltage across the inductor depends on the states of the switching elements. For all three (out of four theoretically possible) combinations of states of switching elements that occur during the converter operation, voltages across the inductor are

$$v_L = \begin{cases} V_{IN} - V_{OUT}, & \text{S - on, D - off} \\ -V_{OUT}, & \text{S - off, D - on} \\ 0, & \text{S - off, D - off} \end{cases} \quad (2)$$

which results in the waveform of the inductor current in the discontinuous conduction mode as depicted in Fig. 3. In the case of the discontinuous conduction mode, later to be labeled as period-1 discontinuous conduction mode, initial value of the inductor current at the beginning of the switching period is zero. The waveform consists of linear segments, since all of the voltages that might appear across the inductor are assumed as constant in time.

C. Normalization

The approach to analyze the switching cell in this paper is primarily based on numerical simulations. To generalize the results, normalization is performed. Choice of the normalization variables is typical, such that all of the voltages are normalized taking the input voltage as the base quantity,

$$m \triangleq \frac{v}{V_{IN}} \quad (3)$$

which results in $M_{IN} = 1$. Chosen notation is such that indexes of the voltages in general remain, while the quantity is labeled as m instead of v . The only exception from this rule is the output voltage, labeled just as M , according to

$$M \triangleq \frac{V_{OUT}}{V_{IN}}. \quad (4)$$

Currents are normalized using $V_{IN}/(f_S L)$ as the base quantity

$$j \triangleq \frac{f_S L}{V_{IN}} i \quad (5)$$

while the time intervals are normalized taking the switching period as the base quantity

$$\tau \triangleq \frac{t}{T_S}. \quad (6)$$

After the normalizations are performed, the differential equation that governs the inductor current reduces to

$$\frac{dj_L}{d\tau} = m_L \quad (7)$$

and the set of possible voltages across the inductor is

$$m_L = \begin{cases} 1 - M, & \text{S - on, D - off} \\ -M, & \text{S - off, D - on} \\ 0, & \text{S - off, D - off} \end{cases} \quad (8)$$

III. DISCRETE TIME MODEL OF THE SWITCHING CELL

Discrete time model of the switching cell is aimed towards obtaining the average the output current of the switching cell during one switching period (j_{OUT}), as well as the final value of the inductor current at the end of the switching period, $j_L(1)$, which is the initial value for the next switching period. Both of the variables are dependent on the initial value of the inductor current, $j_L(0)$, specified maximum of the inductor current when the switch turns off, J_m , and the output voltage, M . To perform the analysis, it is assumed that the output voltage of the switching cell, M , is constant during a switching period.

Operation of the switching cell during a switching period is analyzed following state changes of the switching elements in time, and thus related changes in the inductor voltage.

Each switching period begins with turning the switch on, and the switching cell enters the state when the switch is on, while the diode is off. Assuming this state throughout the switching period, the final value of the inductor current would be

$$j_X = j_L(0) + (1 - M). \quad (9)$$

In the case $j_X \leq J_m$, this completes the switching cycle, and

$$j_L(1) = j_X \quad (10)$$

while contribution of the switching period to the output charge, i.e. the average of the output current is

$$j_{OUT} = \frac{j_L(0) + j_X}{2}. \quad (11)$$

This situation is depicted in Fig. 4(a). In the case $j_X > J_m$, at

$$\tau_1 = \frac{J_m - j_L(0)}{1 - M} \quad (12)$$

the inductor current reaches J_m , and the switch is turned off. The switching cell enters state when the switch is off, and the

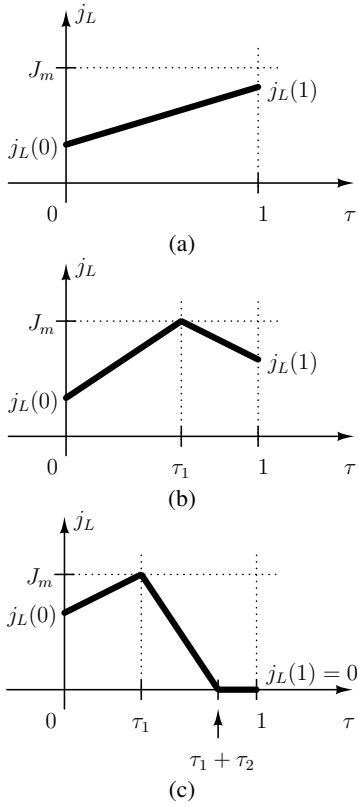


Fig. 4. Switching patterns.

diode is on. Contribution of this interval to the output charge is

$$q_1 = \frac{j_L(0) + J_m}{2} \tau_1. \quad (13)$$

In the second interval, if entered, the inductor current is determined by

$$j_L(\tau) = J_m - M (\tau - \tau_1). \quad (14)$$

Assuming the switching cell remains in this state till the end of the switching period, the final value of the inductor current would be

$$j_Y = J_m - M (1 - \tau_1). \quad (15)$$

In the case $j_Y \geq 0$, obtained value really is the final value

$$j_L(1) = j_Y \quad (16)$$

and contribution of this interval to the output charge is

$$q_2 = \frac{J_m + j_Y}{2} (1 - \tau_1) \quad (17)$$

resulting in the output current

$$j_{OUT} = q_1 + q_2. \quad (18)$$

This situation is depicted in Fig. 4(b). In the opposite case, when $j_Y < 0$, at

$$\tau_2 = \tau_1 + \frac{J_m}{M} \quad (19)$$

the diode turns off. Contribution of the time interval when the diode was on to the output charge is

$$q_3 = \frac{J_m}{2} (\tau_2 - \tau_1). \quad (20)$$

The third interval, if entered, is characterized by $j_L = 0$, since both the switch and the diode are open. This results in the final value of the inductor current

$$j_L(1) = 0 \quad (21)$$

and the output current

$$j_{OUT} = q_1 + q_3. \quad (22)$$

This concludes the switching cell discrete time model. The model should be considered as a mapping of $j_L(0)$, M , and J_m to $j_L(1)$ and j_{OUT} . Although it is possible to provide these two expressions in a closed form, it is avoided here, since the approach that involves auxiliary variables is more convenient to be programmed, and the aim of this paper is semi numerical analysis of the converter, being performed by a computer program. The program used to analyze the buck converter switching cell operated using peak limiting current mode control is given in the Appendix.

IV. CONDUCTION MODES

Under the term ‘‘discontinuous conduction mode’’, period-1 discontinuous conduction mode is frequently assumed [1]. This mode results in the inductor current waveform as shown in Fig. 3, and in the (M, J_m) plane occurs for

$$J_m < M (1 - M) \quad (23)$$

as detailed in [8] using the same notation as in this paper. Besides, the open loop averaged model is unstable for $M > 1/2$, but in the whole region the DCM is characterized by period-1 operation, with stable limit cycle.

As an auxiliary result of [8], occurrence of multiple-period discontinuous conduction modes is described. Such modes are characterized by a waveform which repeats after an integer number of periods, and ends with a period of the type depicted in 4(c), ending by an interval in which the inductor current is equal to zero. Actually, this interval enforces periodical behavior, since the initial condition is exact and fixed.

A question that naturally arises is a range in (M, J_m) plane in which multiple period discontinuous conduction modes occur. A boundary is determined with J_m value which is large enough to guarantee that the inductor will not get discharged over a switching period. Since the inductor is being discharged with the slope $-M$, and the change in the inductor current is $-J_m$ over normalized time $\Delta\tau = 1$, the upper boundary is determined by $J_m = M$. To summarize, conditions for the multiple period discontinuous conduction mode to occur are:

- 1) $J_m > M (1 - M)$, to exclude period-1 discontinuous conduction mode;
- 2) $M > \frac{1}{2}$, to provide unstable limit cycle of period-1 continuous conduction mode, as discussed in [8];
- 3) $J_m < M$, to allow the inductor current to discharge.

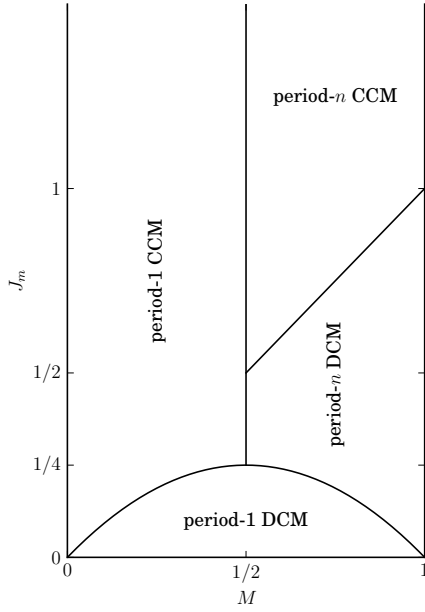


Fig. 5. Chart of the conduction modes.

Described region of operation is depicted in Fig. 5. Besides the described multiple period discontinuous conduction mode, common period-1 discontinuous conduction mode operating region is presented, as well as the continuous conduction modes:

- 1) period-1 continuous conduction mode, for $J_m > M(1 - M)$ (to avoid the discontinuous conduction mode), and $M < \frac{1}{2}$, to provide stable period-1 limit cycle.
- 2) period- n continuous conduction mode, for $J_m > M(1 - M)$, and $M > \frac{1}{2}$, characterized by an unstable limit cycle; it should be noticed that n in “period- n ” might go to infinity ($n \rightarrow \infty$), which corresponds to chaotic operation.

V. OUTPUT CURRENT AND STABILITY

Essential function to be modeled is dependence of the switching cell output current, which is the average of the inductor current, $j_{OUT} = \overline{j_L}$, on the output voltage M , and the control parameter J_m . Under the assumption that the limit cycle is always period-1 and stable, there are two results, depending on the conduction mode:

- 1) in the discontinuous conduction mode the output current is given by

$$j_{OUT} = \frac{J_m^2}{2M(1-M)} \quad (24)$$

- 2) in the continuous conduction mode the output current is given by

$$j_{OUT} = J_m - \frac{1}{2}M(1-M). \quad (25)$$

both of the equations reduce to $j_{OUT} = \frac{1}{2}J_m$ at the boundary between the modes. It should be underlined here that in both of

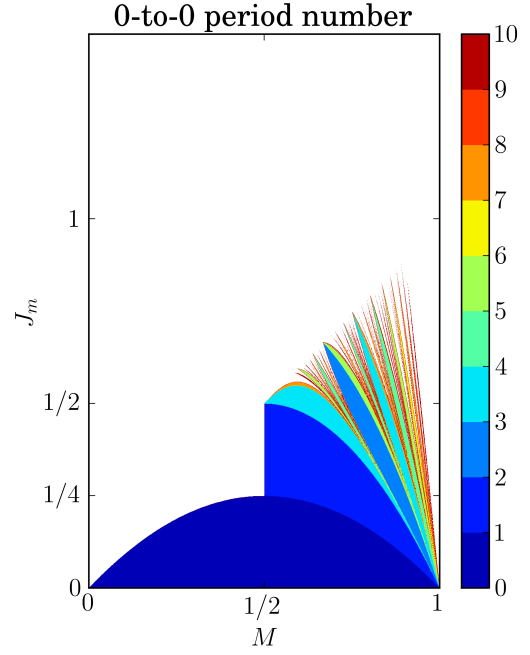


Fig. 6. Dependence of the period number on M and J_m .

the assumed modes the equations are symmetric to the $M = \frac{1}{2}$ line, since the same output current is obtained for M_x and $1 - M_x$, assuming the same value of J_m . This result is revisited in this paper and it is shown that it is wrong, due to the limit cycle instability for $M > \frac{1}{2}$.

For $M > \frac{1}{2}$ the result for the output current for $M > \frac{1}{2}$ and $J_m > M(1 - M)$, is different than given by (25), since the expected inductor current waveforms do not correspond to a stable limit cycle and do not appear in practice. Due to the unstable limit cycle in the continuous conduction mode, the switching cell might operate either in theoretically unlimited number of different period- n discontinuous conduction modes, or in period- n continuous conduction modes and chaotic, i.e. aperiodic, continuous conduction modes, in regions specified in Fig. 5. Dependence of j_{OUT} on M and J_m in such cases is convenient to be analyzed numerically, applying a program given in the Appendix.

The program to analyze the switching cell normalized model numerically, given in the Appendix, iterates the discrete time model of the switching cell for a given set of M and J_m values, starting from the initial value of the inductor current equal to zero. The number of iterations is limited to 500 in the given example, but any larger number would provide even more accurate results. The output current is computed during the simulation, and the output charge accumulated. If at a switching period the converter enters an interval when both the switch and the diode are off, as depicted in Fig. 4(c), the simulation stops, records the period number, and computes the output current according to the charge passed to the output and the number of periods. In the case converter operates in the continuous conduction mode, the simulation

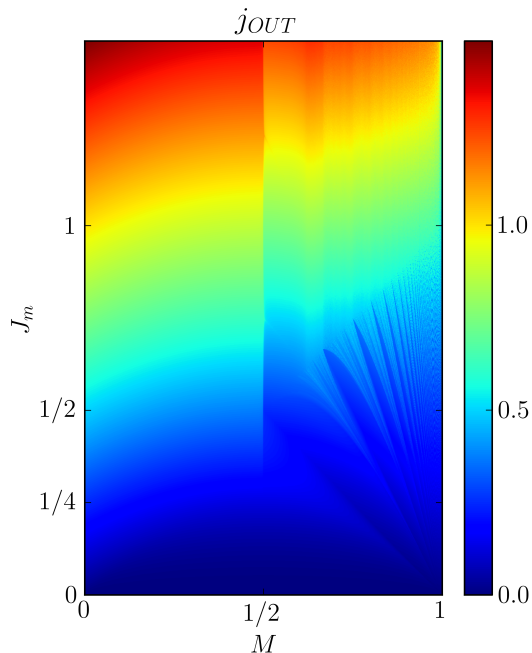


Fig. 7. Dependence of j_{OUT} on M and J_m .

stops after the maximal number of periods elapsed, and the output current is determined as the charge supplied to the output over the interval of time determined by the maximal number of periods. In the continuous conduction modes, the larger the maximal number of periods is, the more accurate value for the output current is obtained, since the startup transient is included in the simulation, not just the steady state operation. Program given in the Appendix is written in Python programming language, using PyLab environment, and presents a core part of the package used to generate results for this paper: it computes and stores the period number and average of the output current. The results are presented in Fig. 6 for the period number and in Fig. 7 for the output current. The diagram of the period number indicates boundary of the continuous conduction mode as predicted in Fig. 5 and by the analysis behind it. The dependence of j_{OUT} on M and J_m does not follow the symmetry predicted by (25) and (24), since instability of assumed fixed points is taken into account.

In [8], focus of the analysis was in period-1 discontinuous conduction mode, where the limit cycle is stable, but the converter is open loop unstable. Term “open loop” assumes constant J_m , not dependent on M . Open loop instability occurs when

$$\frac{dj_{OUT}}{dM} > 0 \quad (26)$$

as detailed in [8]. It is a phenomenon different than the limit cycle instability. For example, for $M > \frac{1}{2}$ and $J_m < M(1 - M)$, the limit cycle is stable, in period-1 discontinuous conduction mode, while the converter is open loop unstable. To analyze stability for $M > \frac{1}{2}$ and $J_m > M(1 - M)$ numerical results provided by the program given in the Ap-

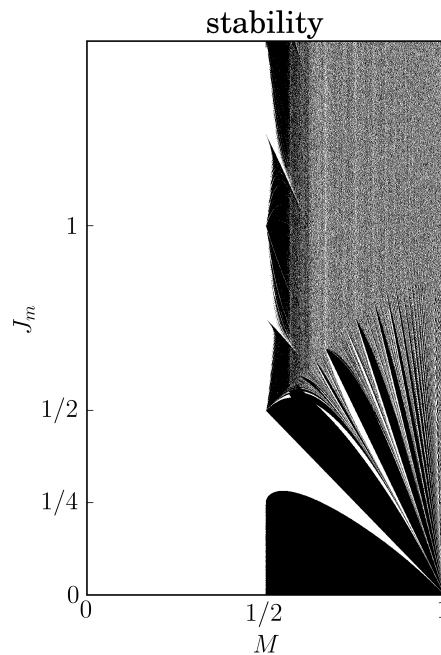


Fig. 8. Dependence of the switching cell open loop stability on M and J_m : white—stable; black—unstable.

pendix are analyzed to determine open loop stability of the converter. Such analysis requires derivative of j_{OUT} over M assuming J_m constant. The analysis is performed over the entire set of simulation results applying finite differences to estimate the derivative numerically. The result is presented in Fig. 8, where open loop stable regions are shown in white, while unstable regions are in black. The results match the theoretical predictions for regions where period-1 operation occurs, both for the continuous and for the discontinuous conduction mode, and provide new insight for limit-cycle unstable regions. Frequent changes from stable to unstable operation indicate that small-signal parameters, commonly used in regulator design, are of limited value in limit cycle unstable regions, due to the sensitivity on parameter variations.

VI. CONCLUSIONS

In this paper, operation of peak limiting current mode control operated buck converter is analyzed, aiming understanding of its operation in unstable limit cycle regions. The converter is analyzed assuming constant output voltage, effectively reducing the converter to the switching cell. Equations of the switching cell are normalized, to generalize the numerical results. A discrete time model of the switching cell is obtained in the form of two functions that map the initial value of the inductor current at the beginning of the switching cycle, the output voltage and the limiting current to the final value of the inductor current at the end of the switching cycle and the average of the inductor current during the switching cycle.

After the normalized model of the switching cell is obtained, it is analyzed assuming period-1 stable limit cycle operation, and boundary between the continuous and the discontinuous

conduction mode is derived, as well as the output current in both of the modes. The result indicates that the dependence of the output current is symmetric over the line determined by the output voltage being equal to one half of the input voltage. Knowing that the limit cycle is unstable for the output voltage greater than one half of the input voltage, boundary of the region where period- n discontinuous conduction modes might occur is determined analytically. Chart of modes is presented in the limiting current versus output voltage plane.

After the analytical approach, numerical methods are applied to analyze the converter. Obtained normalized model of the switching cell is simulated using the program given in the Appendix, and dependence of the output current and the period number on specified values of the output voltage and the limiting current are obtained. Open loop stability of the converter is analyzed, and complex behavior in regions characterized by unstable limit cycle is observed. In regions characterized by stable limit cycle, numerical and analytical results match perfectly. Expected symmetry of the output current assuming stable limit cycle is shown not to occur, and the output current obtained in regions where period-1 limit cycle is unstable is different from the value obtained assuming stability.

Two notions of stability, the limit cycle stability and the open loop stability, are clarified to be different. Open loop stability chart of the converter is presented, showing that all four combinations of the open loop and the limit cycle stability actually occur in the analyzed converter. In regions where the limit cycle is unstable the converter exposes complex behavior, and small signal analysis is of small practical value due to the sensitivity of parameter variations.

REFERENCES

- [1] R. W. Erickson, D. Maksimović, *Fundamentals of Power Electronics*, 2nd Ed., Kluwer, Norwell, MA, 2001.
- [2] C. W. Deisch, "Simple switching control method changes power converter into a current source," *IEEE PESC'78*, 1978, pp. 300–306.
- [3] F. D. Tan, R. D. Middlebrook, "A unified model for current-programmed converters," *IEEE Transactions on Power Electronics*, vol. 10, pp. 397–408, July 1995.
- [4] J. Sun, D. M. Mitchell, M. F. Greuel, P. T. Krein, R. M. Bass, "Modeling of PWM converters in discontinuous conduction mode — A reexamination," *IEEE PESC'98*, 1998, pp. 615–622.
- [5] D. Maksimović, S. Čuk, "A unified analysis of PWM converters in discontinuous modes," *IEEE Transactions on Power Electronics*, vol. 6, pp. 476–490, May 1991.
- [6] T. Sunito, "Analysis and modeling of peak-current-mode-controlled buck converter in DICM," *IEEE Transactions on Industrial Electronics*, vol. 48, February 2001, pp. 127–135.
- [7] C.-C. Fang, "Unified discrete time modeling of buck converter in discontinuous mode," *IEEE Transactions on Power Electronics*, vol. 26, pp. 2335–2342, August 2011.
- [8] M. Glišić, P. Pejović, "Stability Issues in Peak Limiting Current Mode Controlled Buck Converter," *17th International Symposium on Power Electronics Ee 2013*, Novi Sad, October–November 2013

VII. APPENDIX

```
from pylab import *
```

```
nitmax = 500
scale = 1000
```

```
nm = 1 * scale
```

```
deltam = 0.5 / nm
nj = 3 * scale / 2
deltaj = 1.5 / nj
```

```
M = linspace(deltam, 1 - deltam, nm)
Jm = linspace(deltaj, 1.5, nj)
```

```
Jout = empty((nm, nj))
Pern = empty((nm, nj))
```

```
mout = []
jout = []
pern = []
```

```
ijm = - 1
for jm in Jm:
    ijm += 1
```

```
im = - 1
for m in M:
    im += 1
```

```
print jm, m
```

```
# initialization
tau = [0]
jln = [0]
dcmflag = 0
j10 = 0
q = 0
nper = 0
```

```
count = 0
while (dcmflag == 0 and count < nitmax):
```

```
    count += 1
    nper += 1
    tau1 = (jm - j10) / (1 - m)
    if tau1 > 1:
        j11 = j10 + 1 - m
        tau.append(tau[-1] + 1)
        jln.append(j11)
        q += (j10 + j11) / 2.0
        j10 = j11
```

```
    else:
        tau.append(tau[-1] + tau1)
        jln.append(jm)
        q += (j10 + jm) / 2.0 * tau1
        tau2 = jm / m
        if tau1 + tau2 > 1:
            tau3 = 1 - tau1
            j11 = jm - m * tau3
            tau.append(tau[-1] + tau3)
            jln.append(j11)
            q += (jm + j11) / 2.0 * tau3
            j10 = j11
```

```
    else:
        tau.append(tau[-1] + tau2)
        jln.append(0)
        q += jm / 2.0 * tau2
        dcmflag = 1
        tau4 = 1 - tau1 - tau2
        tau.append(tau[-1] + tau4)
        jln.append(0)
        j10 = 0
```

```
jout = q / nper
```

```
Jout[im, ijm] = jout
Pern[im, ijm] = nper
```

```
np.save('M.npy', M)
np.save('Jm.npy', Jm)
np.save('Jout.npy', Jout)
np.save('Pern.npy', Pern)
```